Nanoscale patterning in high resolution HSQ photoresist by interferometric lithography with tabletop extreme ultraviolet lasers

P. W. Wachulak
NSF ERC for Extreme Ultraviolet Science and Technology and Department of Electrical and Computer Engineering, Colorado State University, Fort Collins, Colorado 80523

M. G. Capeluto
Departamento de Física, Facultad de Ciencias Exactas, Universidad de Buenos Aires, 1428 Buenos Aires, Argentina

M. C. Marconi,[a] D. Patel, C. S. Menoni, and J. J. Rocca
NSF ERC for Extreme Ultraviolet Science and Technology and Department of Electrical and Computer Engineering, Colorado State University, Fort Collins, Colorado 80523

(Received 7 June 2007; accepted 1 October 2007; published 7 December 2007)

Arrays of nanodots and nanoholes were patterned with a highly coherent tabletop 46.9 nm laser on high resolution hydrogen silsesquioxane photoresist using multiple exposure interferometric lithography. The authors observed for $\lambda = 46.9$ nm radiation a penetration depth in excess of 150 nm. This laser-based extreme ultraviolet interferometric setup allows printing of 0.5×0.5 mm^2 areas with different nanoscale patterns using a compact tabletop system and exposure times of tens of seconds. © *2007 American Vacuum Society.* [DOI: 10.1116/1.2801870]

I. INTRODUCTION

Hydrogen silsesquioxane (HSQ) has been extensively used as a negative tone photoresist for e-beam lithography, with a demonstrated spatial resolution around 10–12 nm.[1,2] HSQ was also investigated for its applicability in photolithography. The behavior of the resist under the illumination with different wavelengths was previously studied, concluding that HSQ is nonsensitive to visible and UV light down to 193 nm. However, at 157 nm lithographic activity was observed with rather high photon doses, starting at 650 mJ cm^{-2}. With $\lambda = 13.5$ nm extreme ultraviolet (EUV) radiation the onset of negative tone behavior was first reported to start at doses around 50 mJ cm^{-2} (Ref. 3) and in a later experiment at 11.5 mJ cm^{-2}.[4]

The advantage of this inorganic resist, as compared with carbon-based photoresists, is its lower attenuation in the EUV region where all organic materials exhibit strong atomic absorption. This characteristic makes HSQ an attractive alternative as a high resolution photoresist, although the tests performed so far indicate that HSQ is not sensitive enough for mainstream lithographies that would need activation energies below 10 mJ cm^{-2}.

In this paper, we report the fabrication of arrays of nanodots and nanoholes in HSQ coated wafers using multiple exposure interferometric lithography (IL) in a tabletop setup based on a compact $\lambda = 46.9$ nm capillary discharge laser.[5,6] This compact setup enabled the printing of arrays of different motifs using exposure times of few minutes over areas of approximately 500×500 μm^2. The ability to efficiently generate high contrast interference patterns capable to activate in short exposure times the photoresist relies in the high coherence and high brightness of the capillary discharge EUV laser utilized in this experiment. We tested HSQ with the tabletop laser and found that lithographic activity starts at doses around 14 mJ cm^{-2}.

II. EXPERIMENTAL SETUP

The strategy we utilized to print nanoscale periodic features is interferometric lithography. This photolithographic technique is a maskless approach and the patterning is achieved by activating the photoresist with the interference pattern generated by two or more overlapping spatially coherent beams. The main advantages of IL as compared with conventional projection systems are that the spatial resolution is only limited by the wavelength and that it does not depend on the expensive and sophisticated optics necessary to project sub-50 nm features.

The compact Ne-like Ar capillary discharge laser used in this experiment was configured to produce pulses with an energy of approximately 0.1 mJ and about 1.2 ns full width at half maximum (FWHM) duration. It can be operated at repetition rates of several hertz producing EUV powers in excess of 1 mW with high degree of spatial and temporal coherence. The laser operates in the 46.9 nm $3s\,^1P_1 - 3p\,^1S_0$ transition of neonlike Ar. An alumina capillary 3.2 mm in diameter and 28 cm in length filled with Ar is excited with a current pulse of approximately 24 kA, a 10%–90% rise time of approximately 25 ns and a first half-cycle duration of approximately 110 ns.[5,6] To generate the excitation current pulse a four stage Marx generator charged at voltages around 47 kV is used. The current pulse is produced by discharging a water dielectric capacitor through a spark gap switch connected in series with the capillary. The current pulse compresses the plasma column achieving a dense and

[a]Electronic mail: marconi@engr.colostate.edu

hot filamentary plasma channel where a population inversion is created by electron impact excitation of the laser upper level and rapid radiative relaxation of the laser lower level.[7,8] A continuous flow of Ar is injected on front of the capillary to maintain an optimum Ar gas pressure of 490 mTorr in the capillary channel. The spatial intensity distribution in the laser beam has an annular shape with a minimum of approximately 30% of the peak intensity. This annular shape is the result of refraction of the amplified rays in the plasma column due to a plasma density gradient in the radial direction.[6] The peak to peak beam divergence is approximately 4 mrad and the laser emits unpolarized light. For the laser configuration utilized in this experiment, the coherence radius is $\approx$0.6 mm at 1.8 m from the capillary exit.[9,10] This value can be increased by increasing the length of the capillary plasma.[10,11] Considering that the bandwidth of our source is $\lambda/\Delta\lambda \approx 10^4$, the longitudinal coherence length is $\approx$0.470 mm.

The IL setup used in this work has a similar configuration to that reported in a previous experiment in which arrays of cone-shaped nanodots were printed in polymethylmethacrylate (PMMA).[12] In this previous experiment, the shallow penetration depth of the laser light in the PMMA limited the height of the nanodots to 20 nm or so. This problem is overcome using Si based HSQ as the printing photoresist. The setup, described in more detail in Ref. 12, consists of a flat mirror in Lloyd's configuration illuminated with the laser output. Part of the laser beam is reflected in the mirror and interferes with the remaining undeflected portion of the beam, generating interference lines parallel to the mirror's edge, as illustrated in Fig. 1. After the first exposure, the sample was rotated 90° and exposed again to obtain the two dimensional (2D) patterns. This procedure was carried out without necessity to break vacuum, thus assuring similar conditions in both exposures. Figure 1 also shows a photograph of the device with the motorized translation and rotation stages necessary to make the double exposures. The Lloyd mirror interferometer system is housed in a vacuum chamber $0.45 \times 0.55 \times 0.40$ m^3 that was differentially pumped with respect to the laser to maintain a pressure of approximately 10^{-5} Torr. The entire EUV patterning instrument has a footprint of 0.7×2.6 m^2.

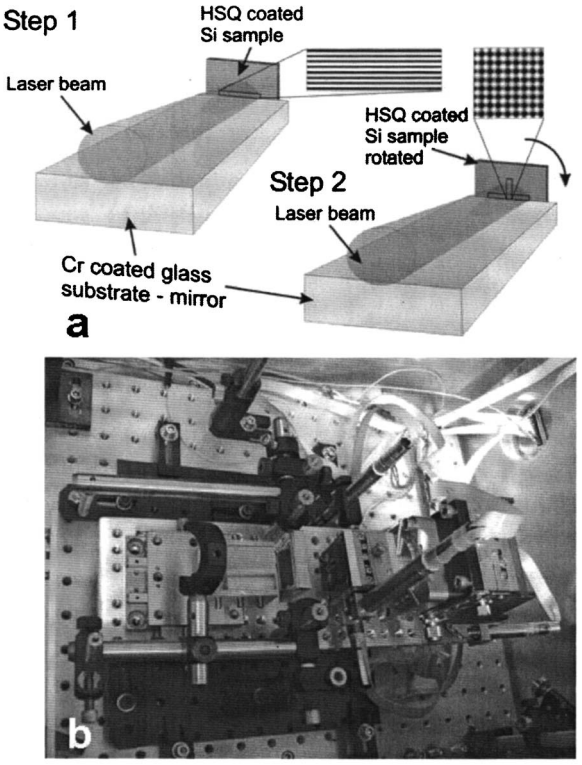

FIG. 1. (a) Two step exposure in Lloyd's mirror IL setup. The sample is rotated an arbitrary angle to obtain different motifs with feature size in the sub-100 nm range. (b) Photograph of Lloyd's mirror device.

III. ANALYSIS OF PHOTOSENSITIVITY OF HSQ AT 46.9 nm

To evaluate the exposure conditions necessary to activate HSQ, we prepared samples consisting of Si wafers spin coated with HSQ at different concentrations. Several Si wafers were spun with HSQ 1% solids, 4% solids, and 6% solids obtaining resist thickness ranging from 35 to 150 nm, which is in good agreement with the spinning curves published by the photoresist's manufacturer.[13] The spinning parameters for the different samples are summarized in Table I. After spinning, the samples were prebaked for 5 min at 90 °C. The samples were exposed with different doses and after the exposure postbaked for 15 min at 110 °C. The developing was performed in LDD26W, 2.38% tetramethylammonium hydroxide (TMAH) in water for 45 s, rinsed with de-ionized water, and dried with nitrogen gas. Table II summarizes the results of this test. An average exposure of 100 laser shots that corresponds to a dose in the sample surface of approximately 35 mJ cm^{-2} completely activates the HSQ. The dose applied was calculated considering the measured photon flux for the laser configuration used in this experiment. We utilized for this measurement a calibrated vacuum photodiode with an Al cathode. The sample was illuminated with a small section of the laser beam corresponding to the maximum intensity in the beam profile. Based on the statistical shot to shot variation of the laser pulse energy we estimate that the exposure dose has an uncertainty of 12%.[6]

This test also demonstrated that the penetration depth of the $\lambda = 46.9$ nm photons is at least 150 nm. This higher penetration depth, as compared with PMMA, will allow printing nanometer size features with high aspect ratio.

TABLE I. Final photoresist thickness obtained for different HSQ concentrations and spinning parameters.

HSQ concentration	Spinning velocity (rpm)	Resist layer thickness (nm)
1% solids	1500	35
4% solids	2000	100
4% solids	3500	75
6% solids	2000	150
6% solids	3500	115

TABLE II. Modulation depth, measured as the difference between the maximum and minimum heights in the photoresist surface for different HSQ concentrations and photon doses.

HSQ concentration	Exposure (mJ cm^{-2})	Modulation depth (nm)
1% solids	30	33
1% solids	60	40
1% solids	90	40
4% solids	30	101
4% solids	45	107
6% solids	30	153
6% solids	45	153

IV. DEMONSTRATION OF MULTIPLE EXPOSURE IL WITH HSQ

Multiple exposure IL was implemented with the HSQ coated samples. We observed that changing the photon flux applied in each exposure allows printing different features. For high photon flux (approximately 14 mJ cm^{-2}) the resist is activated in wide strips that develop in the intersection small holes. Figure 2(a) is an atomic force microscope (AFM) scan showing a 4×4 μm^2 section of an array of holes 130 nm FWHM and 100 nm deep patterned with this high flux. Reducing the flux to approximately 3.5 mJ cm^{-2} the photoresist is only activated in small volumes in the intersections of the fringes corresponding to the maxima of interference, developing in this case an array of small dots, as shown in Fig. 2(b). The versatility of this IL setup allows changing the feature (holes or dots) very easily by changing the applied photon flux and the periodicity by changing the incidence angle on the mirror. The size and distribution of the holes and nanodots in the array were very homogeneous, as can be observed in the 2D Fourier transform of the AFM image. This plot, shown in Fig. 2(c), has only significant contributions at the hole spacing spatial frequency and its harmonics.

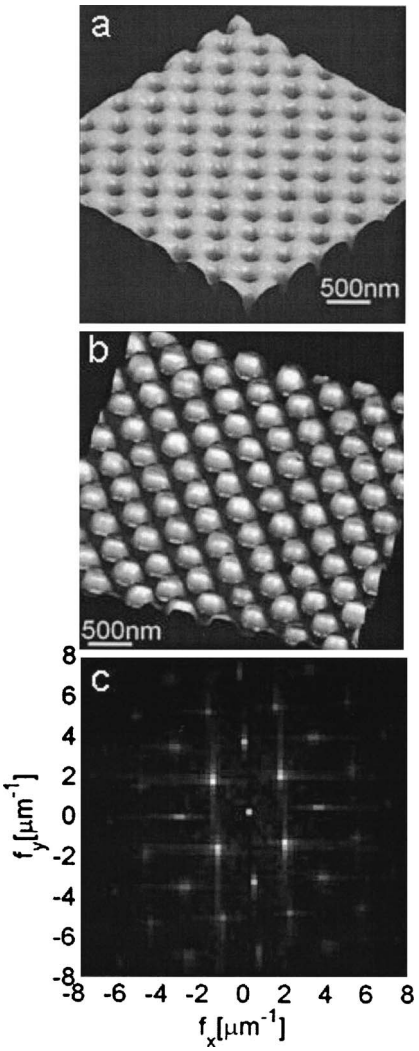

FIG. 2. (a) Array of holes 130 nm FWHM and 100 nm deep developed in HSQ with a high dose illumination. (b) Array of nanodots obtained with low dose illumination. (c) Two dimensional Fourier transform of the image (a) showing only significant contributions at the hole spacing spatial frequency and its harmonics.

We observed that the modulation depth that can be obtained in the exposed HSQ, measured as the difference between the maximum and minimum heights in the photoresist surface, depends on the applied dose at the surface of the photoresist and also on the developing time. Figure 3 is a plot of the modulation depth in a double exposure sample for different exposure and developing conditions. These curves were obtained for a resist layer $\sim$100 nm thick, 4% solution (solids). The applied laser photon fluxes correspond to 8.5, 10.6, 12.8, and 14.5 mJ cm^{-2} for a sample printed with holes with a period of approximately 500 nm. The maximum modulation depth was obtained with a flux in the beam of 8.5 mJ cm^{-2}. This flux corresponds to a dose equivalent to 33 mJ cm^{-2} measured at the resist surface, due to the intensity enhancement produced by the interference effect. To calculate the interference enhancing factor the reflectivity of the mirror at $\theta=2.8°$, the incidence angle used in this test, was assumed to be 96%.[14] For this dose the optimum developing time is between 10 and 20 s with 2.38% concentration of TMAH. These curves indicate that at the lowest flux (8.5 mJ cm^{-2}), the photoresist is not completely activated and it is completely removed by the TMAH solution when the developing time is prolonged more than the optimum developing time. In the regions corresponding to the minima of interference, the low flux assures that the photoresist is completely removed even for short developing times, thus achieving the maximum modulation depth. At larger doses the optimum developing time increases, but also a lower modulation depth is obtained indicating an overexposure of the resist. This can be produced by a partial activation of the photoresist in the regions corresponding to the interference minima, which are not null due to the difference in intensities between the two interfering beams. This effect produces an even dissolution on the polymer layer in the TMAH, obtaining an increasingly lower modulation depth.

The contrast attainable by interferometric lithography also depends on the relative intensity of the two interfering beams that sets the visibility of the interference fringes. In Lloyd's

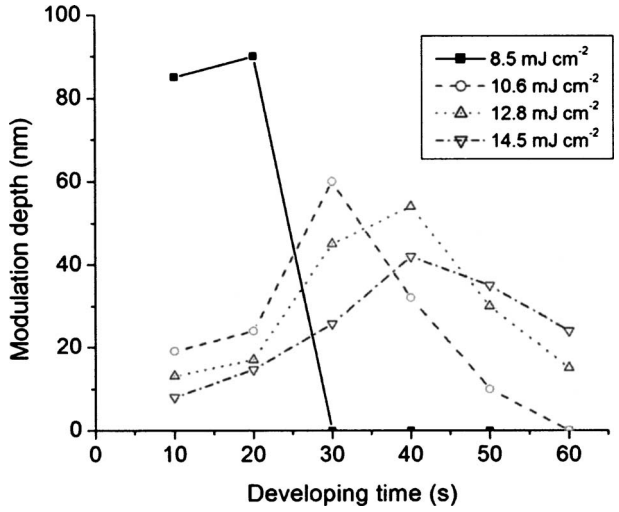

FIG. 3. Modulation depth for an array of holes with ~500 nm period as a function of the developing time for different doses.

mirror configuration one of the beams is reflected, and consequently its intensity is modified by the reflection coefficient of the mirror's surface. In turn, this coefficient depends on the light polarization and the incidence angle. Another factor that can reduce the intensity in the reflected beam is scattering at the mirror's surface. We performed a detailed analysis of these factors in a former experiment.[15] One of the conclusions of this experiment indicated that the loss in contrast due to polarization and angle dependence is only important at incidence angles $\theta > 7°$ that corresponds to patterns period below 200 nm. Also at these larger incidence angles the scattering in the reflecting surface presumably also degrades the reflectivity of the beam. In the present experiment the incident angle in Lloyd's mirror is $\theta = 2.8°$ and consequently we should not expect any significant degradation in the contrast of the interference pattern due to this effect.

V. CONCLUSION

In summary, we have realized nanometer-scale patterning in HSQ using a tabletop system with a tabletop EUV laser and interferometric lithography. Dense arrays of holes and nanodots with a modulation depth of approximately 100 nm were obtained. The periodicity of the structures was controlled by changing the incidence angle of laser beam at the mirror while changing the applied dose and the developing time made possible the printing of holes or dots. We found that HSQ has sensitivity at $\lambda = 46.9$ nm illumination starting the photolithographic activity at doses of approximately 14 mJ cm^{-2} at the surface of the photoresist. We also measured a penetration depth of approximately 150 nm, an almost one order of magnitude larger than the penetration depth obtained at the same wavelength in PMMA. These results show that HSQ holds distinctive advantages when used with EUV photons and is an interesting alternative to realize tabletop nanopatterning with EUV lasers.

ACKNOWLEDGMENTS

This work was supported under the NER program, NSF Award No. DMI-0508484 utilizing facilities from the NSF ERC for Extreme Ultraviolet Science and Technology, Award No. EEC-0310717. M.G.C. acknowledges the support through a fellowship from CONICET.

[1] I. B. Baek, J. H. Yang, W. J. Cho, C. G. Ahn, K. Im, and S. Lee, J. Vac. Sci. Technol. B **23**, 3120 (2005).
[2] H. Yang, A. Jin, Q. Luo, C. Gu, Z. Cui, and Y. Chen, Microelectron. Eng. **83**, 788 (2006).
[3] M. Peuker, M. H. Lim, H. I. Smith, R. Morton, A. K. van Langen–Suurling, J. Romijn, E. W. J. M. van der Drift, and F. C. M. J. M. van Delft, Microelectron. Eng. **61–62**, 803 (2002).
[4] I. Junarsa, M. P. Stoykovich, P. F. Nealey, Y. S. Ma, and F. Cerrina, J. Vac. Sci. Technol. B **23**, 138 (2005).
[5] D. Macchietto, B. R. Benware, and J. J. Rocca, Opt. Lett. **24**, 1115 (1999).
[6] B. R. Benware, C. D. Macchietto, C. H. Moreno, and J. J. Rocca, Phys. Rev. Lett. **81**, 5804 (1998).
[7] J. J. Rocca, Rev. Sci. Instrum. **70**, 3799 (1999).
[8] J. J. Rocca, D. P. Clark, J. L. A. Chilla, and V. N. Shlyaptsev, Phys. Rev. Lett. **77**, 1476 (1996).
[9] The coherence radius R_c define the transverse coherence of the source. R_c is defined following the convention of coherence area $A_c = \pi R_c^2$ given in J. W. Goodman, *Statistical Optics* (Wiley, New York, 1985), pp. 171–187.
[10] Y. Liu, M. Seminario, F. G. Tomasel, C. Chang, J. J. Rocca, and D. T. Attwood, Phys. Rev. A **63**, 033802 (2001).
[11] M. C. Marconi, J. L. A. Chilla, C. H. Moreno, B. R. Benware, and J. J. Rocca, Phys. Rev. Lett. **79**, 2799 (1997).
[12] P. W. Wachulak, M. G. Capeluto, M. C. Marconi, C. S. Menoni, and J. J. Rocca, Opt. Express **15**, 3465 (2007).
[13] http://www.dowcorning.com
[14] Center for X-Ray Optics, http://www-cxro.lbl.gov
[15] M. G. Capeluto, G. Vaschenko, M. Grisham, M. C. Marconi, S. Ludueña, L. Pietrasanta, Y. Lu, B. Parkinson, C. S. Menoni, and J. J. Rocca, IEEE Trans. Nanotechnol. **5**, 3 (2006).